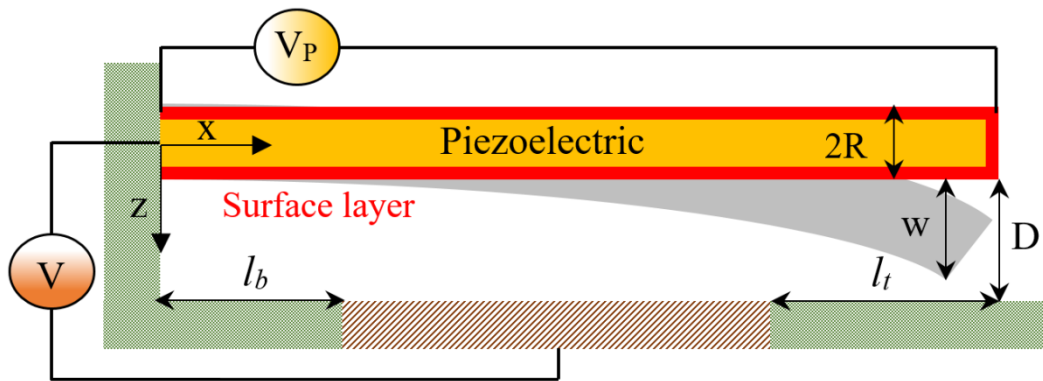**Graphical Abstract**



Providing a general nonlinear model of piezoelectric microwires with the ability in adjusting stability conditions to improve the system characteristics. It was implemented by applying the piezo-voltage and/or actuating just a piece of the substrate electrostatically.

# Nonlinear Stability Analysis of Piecewise Actuated Piezoelectric Microstructures

Masoud SoltanRezaee[a,*], Mahdi Bodaghi[b], Amin Farrokhabadi[c], Reza Hedayati[d]

[a] Young Researchers and Elites Club, Science and Research Branch, Islamic Azad University, Tehran, Iran
([*] Corresponding author. E-mail address: soltanrezaee@gmail.com)
[b] Department of Engineering, School of Science and Technology, Nottingham Trent University, Nottingham NG11 8NS, United Kingdom (mahdi.bodaghi@ntu.ac.uk)
[c] Department of Mechanical Engineering, Tarbiat Modares University, Tehran, Iran (amin-farrokh@modares.ac.ir)
[d] Novel Aerospace Materials group, Faculty of Aerospace Engineering, Delft University of Technology (TU Delft), Kluyverweg 1, 2629 HS Delft, The Netherlands (r.hedayati@tudelft.nl)

**Abstract**     The main objective of this research is to provide a general nonlinear model of adjustable piezoelectric microwires with the ability to tune the stability conditions. In order to increase the controllability and improve system characteristics, only a part of the substrate is electrostatically actuated and the piezoelectric voltage is also applied. The governing equation of equilibrium (EOE) is derived from the principle of minimum total potential energy. The influences of the surface layer, size dependency, piezoelectricity, and dispersion forces are also included simultaneously. To solve the nonlinear differential equation, a numerical method is implemented and the obtained results are validated with available experimental and numerical results. Afterward, a set of parametric studies is carried out to examine the coupled effects of piezo-voltage, length/position of non-actuated pieces, nonlinear curvature, and molecular forces on the microresonators. It is found that the beam deflection and the pull-in voltage have sensitive-dependence on the system behavior. Furthermore, the beam deflection can increase or decrease with consideration of different positions of non-actuated pieces. This research is expected to fill a gap in the state of the art of the piezoelectric microstructures and present relevant results that are instrumental in the investigation of advanced actuated microdevices.

**Keywords** Nonlinear Stability Analysis; Piezoelectric Excitation; Casimir Regime; Micro-Actuators

## 1. Introduction

Along with the developments in the design and production of miniature systems, actuated ultra-small devices are becoming affordable systems with many applications. Exemplary characteristics of micro and nanoelectromechanical systems (M/NEMS) are low weight, high precision, and low energy consumption. Such systems are being appeared in an extensive variety of applications, including sensors/actuators, capacitive switches, smart systems, tunable valves, ultra-sensitive detectors, and biodevices [1-7]. Analyzing the structural behavior and instability conditions of these systems are essential to improve their design and performance [8-15].

The emergence of several substantial influences such as molecular attractions, the surface layer (SL), and material length dependency within the dimension variation causes to various new behaviors that are emerging in ultra-small structures, which are not effective in other dimensions. For example, the intermolecular van der Waals (vdW) and Casimir force have remarkable impacts on the system stability [16, 17]. Such attractions have fundamental influences in the microscale, while they are not considerable in larger scales [18]. To illustrate that molecular forces can shift the stable center point, the bifurcation of circular nanoplates and functionally graded (FG) nanoactuators has recently been investigated by Yang et al. [19] and Esfahani et al. [20]. Another important influence that affects the system behavior and becomes dominant in microstructures is the SL. Recently, the pull-in instability and structural behaviors of microsystems have been

1

examined considering the SL effects [21-23]. Both surface residual stress and surface layer elasticity of electrothermally actuated miniature diaphragms have been evaluated by Yang et al. [19]. Furthermore, the surface layer effects of functionally graded (FG) nanoresonators have been studied to examine their hardening/softening treatment by considering the fraction index [20]. In addition to the intermolecular attractions and SL effects, the length-scale of bulk material in the miniature dimensions can be an elemental effect that must be taken into account. Experimental results disclose that the size effect may change the behavior and responses of microdevices completely [24, 25]. Moreover, the numerical results demonstrate the important effects of length-scale in composite laminated microstructures [23] and FG nanobeams [20] using the differential quadrature method. To model the material length-scale effect in recent studies, non-classical theories were considered, for example, the couple stress (CST) [26], non-local [27] as well as strain gradient [24] theories.

The deformable part of numerous microstructures undergoes relatively considerable deflection that is called the geometrically nonlinear curvature. In addition, different sources of nonlinearity, such as the electrical actuation and molecular attractions exist in miniature devices. For such MEMS with fundamentally nonlinear behavior, except a few approximate analytical solutions, no exact closed-form solutions have been proposed. Anderson et al. [28] experimentally have revealed that neglecting the geometrical nonlinearity affects the system behavior and responses significantly. Dai et al. [29] have analyzed forced vibrations of cantilever nanoswitches by considering nonlinearities in curvature and inertia. Moreover, the effect of an attached particle on the power enhancement of broadband smart energy harvesting has been studied with consideration of both nonlinear inertia and nonlinear curvature by Firoozy et al. [30]. Recently, Fang et al. [31] have focused on size-dependent rotating FG microbeams by considering the geometric nonlinearity. The analysis of nonlinear models [28-31] reveals the importance of accounting the geometric nonlinearity, which affects the stability considerably.

It must be noted that the system configuration is a substantial issue in the simulation of miniature instruments. Recently, vibrations of numerous types of tiny complex constructions and smart systems have been studied [32-35]. Pourkiaei et al. [32, 33] have modeled a double-sided clamped-clamped nanobeam under combined alternating as well as direct current loadings to evaluate parametric resonances using the perturbation method. Furthermore, a pedal from FG materials as a microactuator involving flexural and torsional modes has been modeled by Shoghmand and Ahmadian [35] to investigate softening/hardening treatments. In order to develop the microstructural architecture, various general models must be designed and analyzed in detail. In such devices, for example, the length and/or position of the electrically actuated fixed conductor can be adjustable. As a result, the entire length of the substrate conductor is not stimulated, which can be used as a control parameter in optimization and applied design.

Nowadays, the piezoelectric materials have an important contribution in different intelligent structures as an excitation source with several advantages. Moreover, the ability of piezoelectric material in nonlinear vibration-based piezoelectric energy harvesters has been widely studied [8, 14, 15]. Recently, the static equilibrium, bifurcation points, and parametric resonances of double-clamped pure piezobeams have been examined numerically and semi-analytically by Pourkiaee et al. [32, 33] without modeling the size effect. Moreover, the responses of clamped-clamped nanobeams [21, 23, 36] and microplates [37, 38] with attached piezo-layers have been examined. Numerous researchers have modeled fully clamped structures [21, 23, 32, 33, 36-38], however, despite different applications of cantilever wires, they have less been studied.

The effects of molecular forces, surface layer energy, material length-scale, geometrical nonlinearity, system architecture, and piezoelectricity have been distinctly reviewed. To the best of authors' knowledge, the coupled influences of all these parameters on the nonlinear stability of piezoelectric microstructures have not been examined yet. The motivation of this study is to develop a comprehensive model to investigate the effects of system configuration (position/length of the electrostatically actuated part) and piezoelectric excitation as two major control parameters on the behavior of smart structures. In this study, pull-in characteristics regarding the piezoelectric, electrostatic, and molecular effects are studied in detail. Moreover, the variation of geometrical nonlinearity, surface layer parameters, piezo-voltage, and the length/location of non-actuated pieces of the substrate on the structural behavior are discussed simultaneously for the first time. Owing to lack of similar formulation and results in the specialized literature, they are expected to contribute to a better understanding on the nonlinear stability of piecewise actuated piezoelectric microstructures and would be beneficial to the optimal design of smart systems.

## 2. Theoretical Model

In **Fig. 1**, schematic of a microsystem suspended over a fixed electrode is presented. The actuated microwire deflects down due to the electrostatic and dispersion regimes. In the present microstructure, the terms $L$ and $R$ denote the length and radius of the piezoelectric beam, respectively. Moreover, the term $D$ denotes the primary distance between the electrostatically actuated conductors.

### 2.1. Strain and potential energy

Based on the modified couple stress theory (MCST) [39], which has been able to find acceptable results in the microscale, the strain energy of an ultra-small system is related to the strain and rotation field [40]. Consequently, it is expressed in the microcantilevers as

$U = \mathbf{m} : \mathbf{\kappa} + \mathbf{\sigma} : \mathbf{\varepsilon}$, (1) where, the rotation tensor $\mathbf{\omega}$ and vector $\mathbf{\theta}$ can be mentioned as

$$\omega_{ij} = \left(u_{i,j} - u_{i,i}\right)/2 = -\omega_{ji}, \quad \theta_i = \left(e_{ijk}u_{k,j}\right)/2, \tag{2}$$

where the term $e_{ijk}$ denotes the permutation symbol. By neglecting the beam horizontal displacement $u$ in Eq. (2), it is derived as

$$\omega_{ij} = e_{ijk}\theta_k, \quad \theta_i = \left(e_{ijk}\omega_{jk}\right)/2. \tag{3}$$

Considering the rotation gradient $\mathbf{\kappa}$ and by replacing Eq. (3) into Eq. (1), one obtains

$$\kappa_{ij} = \theta_{j,i} = \left(e_{jkl}\omega_{kl,i}\right)/2 = \left(e_{jkl}u_{l,ki}\right)/2. \tag{4}$$
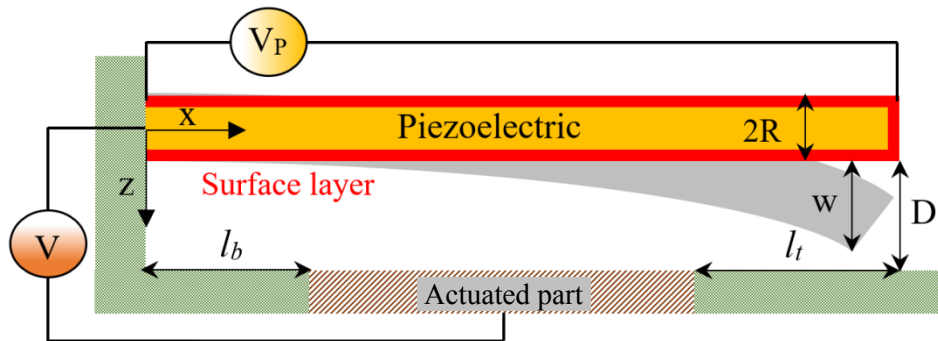


**Fig. 1.** Schematic of the present piecewise actuated piezoelectric microwire

3

In addition, the nonlinear strain tensor $\varepsilon$ can be introduced as

$$\varepsilon_{ij} = \left(2u_{i,j} + u_{k,i}u_{k,j}\right)/2.\tag{5}$$

The strain energy $\underline{u}$ according to the elasticity theory is stated as [41]

$$\underline{u} = \left(\underline{\lambda}/2 + \mu\right)\varepsilon_{ij}\varepsilon_{ij} + 2\left(\phi + \phi'\right)\kappa_{ij},\tag{6}$$

where $\underline{\lambda}$ and $\mu$ introduce Lame's constant and shear modulus, respectively, however, the terms $\phi$ and $\phi'$ are impacts of non-classical theory. Furthermore, the deviatoric tensor $\mathbf{m}$ is expressed as

$$m_{ij} = d\underline{u}/d\kappa_{ij} = 4(\phi\kappa_{ij} + \phi'\kappa_{ji}),\tag{7}$$

where $\phi = \mu l^2$ and $l$ denotes the size dependency. Finally, the terms $\kappa_{ij}$ and $m_{ij}$ are rederived as

$$\kappa_{xy} = -\frac{d^2w}{dx^2};\quad \text{all other}\quad \kappa_{ij} = 0,\tag{8}$$

$$m_{xy} = -4\mu l^2\frac{d^2w}{dx^2}, m_{yx} = -4\left(\mu l^2\right)'\frac{d^2w}{dx^2};\quad \text{all other}\quad m_{ij} = 0.$$

In general, the axial strain of a beam $\varepsilon_0$ at the natural axis is written as

$$\varepsilon_0 = \sqrt{\left(1+\frac{du}{dx}\right)^2 + \left(\frac{dw}{dx}\right)^2} - 1.\tag{9}$$

Furthermore, the nonlinear curvature $\zeta$ is expressed by the following equation [42]

$$\zeta = \left(\left(1+\frac{du}{dx}\right)\frac{d^2w}{dx^2} - \frac{d^2u}{dx^2}\frac{dw}{dx}\right)\left(\left(1+\frac{du}{dx}\right)^2 + \left(\frac{dw}{dx}\right)^2\right)^{2/3}.\tag{10}$$

Initially, there is no strain at the natural axis [42]; accordingly, considering Eq. (10) and $\varepsilon_0 = 0$, one obtains the term $\zeta$ as

$$\zeta = \left(1+\frac{du}{dx}\right)\frac{d^2w}{dx^2} - \frac{d^2u}{dx^2}\frac{dw}{dx}.\tag{11}$$

By applying Taylor's expansion, we have

$$\frac{du}{dx} \approx -\frac{1}{2}\left(\frac{dw}{dx}\right)^2.\tag{12}$$

Accordingly, the term $\zeta$ is rewritten as

$$\zeta = \frac{d^2w}{dx^2} + \frac{1}{2}\left(\frac{dw}{dx}\right)^2\frac{d^2w}{dx^2}.\tag{13}$$

The axial stress and strain of such systems due to the geometrical nonlinearity is stated as

$$\varepsilon_{xx} = \varepsilon_0 - z\zeta;\quad \text{all other}\quad \varepsilon_{ij} = 0,\tag{14}$$

$$\sigma_{xx} = E\varepsilon_{xx} - E_z e_{31};\quad \text{all other}\quad \sigma_{ij} = 0,\tag{15}$$

where $E$, $E_z$, and $e_{31}$ are respectively Young's modulus of the bulk material, electric vector of piezoelectricity, and transversal piezo-coefficient ($= 6.4$ C.m$^{-2}$).

Due to the electromechanical response of piezobeams, a voltage between two ends of the beam can be supposed, see **Fig. 1**. Hence, the strain energy of smart microbeam is expressed as [43]

$$U_P = -e_{31}E_z\frac{A}{2}\int_0^L\left(\frac{dw}{dx}\right)^2 dx.\tag{16}$$

Considering $V_P$ as the piezo-voltage, the piezoelectric field vector can be defined as

$$E_z = V_P/(2R).\tag{17}$$

The tension in the surface layer of the microcantilever is stated as

$$\tau = \tau_0 + E^s \varepsilon_{xx}{}^s,\tag{18}$$

where $\tau_0$ and $E^s$ are respectively the residual stress and the Young modulus of the SL. Accordingly, the moment of the movable electrode is derived as

$$M = \int_A \sigma_{xx} z\,dz + \int_S \left(\tau_0 + E^s \varepsilon_{xx}{}^s\right) z\,dz = -\zeta\left(\pi E R^4/4 + \pi E^s R^3\right).\tag{19}$$

It is worth noting that we suppose the structure to be homogeneous and linear elastic. Therefore, the strain energy can be obtained as

$$U = \frac{1}{2}\int_0^L \left( \zeta^2 \left( \frac{\pi E R^4}{4} + \pi E^s R^3 \right) + 4\mu A l^2 \left( \frac{d^2 w}{dx^2} \right)^2 \right) dx.\tag{20}$$

Owing to the residual stress in the SL, there is another force acting along the deformable electrode as

$$q = 4\tau_0 R\zeta.\tag{21}$$

As a result, the produced energy can be written as

$$V_q = \int_0^L 2\tau_0 R\zeta\, w\,dx.\tag{22}$$

### 2.2. External work

The work of the mentioned forces includes the electrostatic force in addition to the Casimir or vdW attractions can be written by the following equation

$$W_{ext} = \int_0^L F_{ext} w\,dx.\tag{23}$$

The electric attraction with consideration of fringing effect is expressed as [44]

$$F_{els} = \frac{\pi V^2 \varepsilon_0}{(D-w)\operatorname{arccosh}^2 (D-w)/R},\tag{24}$$

where $V$ is the voltage applied between electrodes and $\varepsilon_0 = 8.8\times10^{-12}$ F.m$^{-1}$ is the space permittivity.

In addition, the Casimir attraction between the microwire and substrate is given by [45]

$$E_{cas} = -\frac{PcL}{16\pi D^2 \ln D/R},\tag{25}$$

where $P = 1.055\times10^{-34}$ Js is the reduced Planck constant and $c = 2.99\times10^8$ m/s is the speed of light. By differentiating the energy, the effect of Casimir regime is derived as

$$F_{cas} = \frac{dE_{cas}}{dD} = \frac{Pc}{16\pi(D-w)^3 \ln^2 (D-w)/R}\left(1 + 2\ln\frac{D-w}{R}\right).\tag{26}$$

On the other hand, the vdW attraction between the microwire and substrate is [46]

$$E_{vdw} = -\frac{c_h R^2}{3D^3},\tag{27}$$

where the term $c_h$ denotes the Hamaker's constant that is $4.0\times10^{-19}$ J [47]. Therefore, the vdW force is written as

$$F_{vdw} = \frac{dE_{vdw}}{dD} = \frac{c_h R^2}{D^4}.\tag{28}$$

5

Furthermore, since the electrostatically actuated length of the substrate plate may be shorter than the movable conductor, the microwire will be subjected to the pricewise electrostatic force as well as intermolecular forces. Thus, the external work relationship can be stated as

$$W_{ext} = \int_0^L \left( \int_0^w \left( F_{els} H(x) + \begin{Bmatrix} F_{vdw} \\ F_{cas} \end{Bmatrix} \right) dw \right) dx .$$ (29)

It should be mentioned that the electrically actuated area of the movable conductor can be revealed as

$$H(x) = H(x - l_b) - H(x + l_t - L),$$ (30)

where the terms $l_b$ and $l_t$ are respectively the lengths of the first (base) and the second (tip) pieces of the fixed conductor, as demonstrated in **Fig. 1**.

It is worth noting that by applying the electric potential to a microwire, it deflects down to the substrate plate and their distance is reduced to $D-w$. As a result, external forces can be given as

$$F_{els} H(x) + \begin{Bmatrix} F_{vdw} \\ F_{cas} \end{Bmatrix} = \frac{\pi V^2 \underline{\varepsilon}_0 \left( H(x - l_b) - H(x + l_t - L) \right)}{(D-w)\operatorname{arccosh}^2 (D-w)/R} + \begin{Bmatrix} c_h R^2 \big/ (D-w)^4 \\ \dfrac{cP\left(1 + 2\ln\left((D-w)/R\right)\right)}{16\pi (D-w)^3 \ln^2\left((D-w)/R\right)} \end{Bmatrix}.$$ (31)

### 2.3. *Energy variation*

Having the strain and potential energies of the microcantilever wire as well as external works, the minimum total potential energy principle is implemented as

$$\delta(U + V_q - W_{ext}) = 0.$$ (32)

Substituting Eqs. (16), (20), (22), (29), and (31) into Eq. (32) leads to the governing equilibrium equation as

$$\left( \frac{\pi E R^4}{4} + \pi E^s R^3 \right) \left[ \frac{d^4 w}{dx^4} + \frac{d}{dx}\left( \frac{dw}{dx} \frac{d}{dx}\left( \frac{d^2 w}{dx^2} \frac{dw}{dx} \right) \right) \right] + 4\mu A l^2 \frac{d^4 w}{dx^4}$$

$$+ e_{31} V_P \frac{\pi R}{2} \frac{d^2 w}{dx^2} - 2\tau_0 R \frac{d^2 w}{dx^2}\left( 4 + \left(\frac{dw}{dx}\right)^2 \right) = F_{els} H(x) + \begin{Bmatrix} F_{vdw} \\ F_{cas} \end{Bmatrix};$$ (33)

By substituting $l=0$ in Eq. (33), the non-classical MCST can easily be changed to the classical one. On the other hand, the boundary conditions (BCs) of a cantilever wire are

$$w(0) = 0, \; \frac{dw(0)}{dx} = 0, \; \frac{d^2 w(L)}{dx^2} = 0, \; \frac{d^3 w(L)}{dx^3} = 0.$$ (34)

It is more convenient to express the relationships in nondimensional form by defining the subsequent parameters:

$$\Xi = \frac{x}{L}, \Upsilon = \frac{w}{D}, \psi = \frac{D-w}{D}, \chi = \frac{D}{R}, \mu = \frac{D^2}{L^2}, \upsilon = \frac{2VL}{R^2}\sqrt{\frac{\varepsilon_0}{E}}, \alpha = \frac{4E^s}{ER}, \beta = \frac{4\tau_0 L^2}{E\pi R^3},$$

$$I = \frac{\pi R^4}{4}, \kappa = \frac{16\mu l^2}{ER^2}, p = \frac{l_b}{L}, q = \frac{l_t}{L}, a_{vdw} = \frac{c_h R}{EI}, a_{cas} = \frac{Pc}{16\pi EI}, \nu = \frac{2e_{13} V_P L^2}{ER^3},$$ (35)

$$H(\Xi) = H(\Xi - p) - H(\Xi + q - 1).$$

By substituting the terms in Eq. (35) into Eq. (33), the dimensionless equation is obtained as

$$(1+\alpha)\left[\frac{d^4\Upsilon}{d\Xi^4}+\mu\frac{d}{d\Xi}\left(\frac{d\Upsilon}{d\Xi}\frac{d}{d\Xi}\left(\frac{d^2\Upsilon}{d\Xi^2}\frac{d\Upsilon}{d\Xi}\right)\right)\right]-2\lambda\left(4+\mu\left(\frac{d\Upsilon}{d\Xi}\right)^2\right)\frac{d^2\Upsilon}{d\Xi^2}+\nu\frac{d^2\Upsilon}{d\Xi^2}+\kappa\frac{d^4\Upsilon}{d\Xi^4}$$

$$=\frac{\upsilon^2}{\mu(1-\Upsilon)\operatorname{arccos h}^2(\chi(1-\Upsilon))}H(\Xi)+\left\{\begin{array}{c}\dfrac{a_{vdw}}{\chi\mu^2(1-\Upsilon)^4}\\[4mm]\dfrac{a_{cas}(1+2\ln(\chi(1-\Upsilon)))}{\mu^2(1-\Upsilon)^3\ln^2(\chi(1-\Upsilon))}\end{array}\right.\quad. \tag{36}$$

### 3. Solution Method

In general, analytical methods could not solve the nonlinear differential equation of electrically actuated piezoelectric microstructures. Therefore, the governing equation of equilibrium (EOE) should be linearized and solved numerically. Here, step-by-step linearization method (SSLM) [48] is used to calculate pull-in instability parameters. The solution for considering the bending behaviors of cantilever microbeams is prepared. The vertical deflection of a deformable electrode $\Upsilon$ is mentioned as

$$\Upsilon=\mathbf{B}^T\boldsymbol{\varphi}=\sum_{i=1}^{N}B_i\varphi_i, \tag{37}$$

where $B_i$ denotes the amplitude factor of the beam and

$$\varphi_i(\Xi)=(\sin\vartheta_i\Xi-\sinh\vartheta_i\Xi)\big([\cos\vartheta_i+\cosh\vartheta_i]/[\sin\vartheta_i+\sinh\vartheta_i]\big)+\cosh\vartheta_i\Xi-\cos\vartheta_i\Xi. \tag{38}$$

In order to calculate the values of term $\vartheta_i$, the relationship $\cos\vartheta_i\cosh\vartheta_i=-1$ should be solved.

Eventually, after some straightforward mathematical manipulations, we have

$$n(\mathbf{B})=\big((1+\alpha+\kappa)K_1+(1+\alpha)\mu K_2+(\nu+\beta)K_3+\mu\beta K_4\big)\mathbf{B}, \tag{39}$$

where

$$K_1=\int_0^1\frac{d^2\boldsymbol{\varphi}}{d\Xi^2}\frac{d^2\boldsymbol{\varphi}^T}{d\Xi^2}d\Xi, \tag{40}$$

$$K_2(\mathbf{B})=2\int_0^1\frac{d\boldsymbol{\varphi}}{d\Xi}\frac{d^2\boldsymbol{\varphi}^T}{d\Xi^2}\mathbf{B}\frac{d\boldsymbol{\varphi}^T}{d\Xi}\mathbf{B}\frac{d^2\boldsymbol{\varphi}^T}{d\Xi^2}d\Xi, \tag{41}$$

$$K_3=-\int_0^1\boldsymbol{\varphi}\frac{d^2\boldsymbol{\varphi}^T}{d\Xi^2}d\Xi, \tag{42}$$

$$K_4(\mathbf{B})=-\frac{1}{2}\int_0^1\boldsymbol{\varphi}\frac{d\boldsymbol{\varphi}^T}{d\Xi}\mathbf{B}\mathbf{B}^T\frac{d\boldsymbol{\varphi}}{d\Xi}\frac{d^2\boldsymbol{\varphi}^T}{d\Xi^2}d\Xi, \tag{43}$$

$$n(\mathbf{B})=\int_0^1\left(\frac{\upsilon^2 H(\Xi)}{\mu(1-\boldsymbol{\varphi}^T\mathbf{B})\operatorname{arccos h}^2(\chi(1-\boldsymbol{\varphi}^T\mathbf{B}))}+\left\{\begin{array}{c}\dfrac{a_{vdw}}{\chi\mu^2(1-\boldsymbol{\varphi}^T\mathbf{B})^4}\\[4mm]\dfrac{a_{cas}(1+2\ln(\chi(1-\boldsymbol{\varphi}^T\mathbf{B})))}{\mu^2(1-\boldsymbol{\varphi}^T\mathbf{B})^3\ln^2(\chi(1-\boldsymbol{\varphi}^T\mathbf{B}))}\end{array}\right.\right)\boldsymbol{\varphi}d\Xi. \tag{44}$$

7

The stiffness terms of the micromanipulator $\alpha K_1$, $\kappa K_1$, $\beta(K_3+\mu K_4)$ and $\mu K_2(1+\alpha)$ are the effects of layer elasticity, length-scale, residual stress and nonlinearity, respectively.

Considering Eq. (39), the system stiffness is stated as

$$K = (1+\alpha+\kappa)K_1 + 3(1+\alpha)\mu K_2 + (\nu+\beta)K_3 + 3\mu\beta K_4 - dn(\mathbf{B})/d\mathbf{B},\tag{45}$$

where

$$\frac{dn}{d\mathbf{B}} = \int_0^1 \left( \begin{array}{c} \upsilon^2 H(\Xi) \dfrac{\dfrac{2\chi(1-\boldsymbol{\varphi}^T\mathbf{B})}{\sqrt{(\chi(1-\boldsymbol{\varphi}^T\mathbf{B}))^2-1}\,\operatorname{arccosh}(\chi(1-\boldsymbol{\varphi}^T\mathbf{B}))} + 1}{\mu(1-\boldsymbol{\varphi}^T\mathbf{B})^2 \operatorname{arccosh}^2(\chi(1-\boldsymbol{\varphi}^T\mathbf{B}))} \\[4em] + \left\{ \begin{array}{l} \dfrac{4a_{vdw}}{\chi\mu^2(1-\boldsymbol{\varphi}^T\mathbf{B})^5} \\[2em] a_{cas}\dfrac{2+5\ln(\chi(1-\boldsymbol{\varphi}^T\mathbf{B}))+6\ln^2(\chi(1-\boldsymbol{\varphi}^T\mathbf{B}))}{\mu^2(1-\boldsymbol{\varphi}^T\mathbf{B})^4\ln^3(\chi(1-\boldsymbol{\varphi}^T\mathbf{B}))} \end{array} \right. \end{array} \right) \boldsymbol{\varphi}\boldsymbol{\varphi}^T d\Xi.\tag{46}$$

Deformation of a microcantilever owing to the DC electric potential is determined by solving Eq. (47). Finally, the EOE is formulated as

$$\left((1+\alpha+\kappa)K_1 + 3(1+\alpha)\mu K_2 + (\nu+\beta)K_3 + 3\mu\beta K_4\right)\mathbf{B} = n_{els}H(\Xi) + \left\{ \begin{array}{l} n_{vdw} \\ n_{cas} \end{array} \right..\tag{47}$$

It should be mentioned that the term $\Upsilon^i$ is the nondimensional deformation due to the applied electric potential $\upsilon^i$. By enhancing the electric potential gradually $\upsilon^{i+1} \to \upsilon^i + \delta\upsilon$, the nondimensional wire displacement is obtained as

$$\Upsilon^{i+1} \to \Upsilon^i + \delta\Upsilon.\tag{48}$$

## 4. Results and Discussion

To verify the developed model as well as the solution method, the simulation results are validated with available experiments [49]. Accordingly, the behavior of a fully actuated cantilever wire with a gap of $D = 3$ μm, length of $L = 6.8$ μm, radius of $R = 23.5$ nm, and Young's modulus of $E = 900$ GPa is investigated (the relationships of external works, as well as relevant constants, have been presented in Section 2.2). Note that in the considered carbon-based electrode, the molecular parameters do not play significant roles on the pull-in instability. This fact has been demonstrated analytically [49] and numerically [50-53], so their effects can be ignored. The comparison between the instability characteristics achieved by our proposed model is made with measured results as illustrated in **Fig. 2**. In this figure, the vertical axis displays the distance between the beam tip and the substrate, see **Fig. 1**. Furthermore, the horizontal axis displays the DC applied voltage V that increases gradually. The present model and solution predict the pull-in voltage as 48.51-Volt that is very close to the measured 48-Volt [49]. Moreover, the comparison of the instability voltages calculated by the present method with respect to other numerical methods as reported in Ref. [50-53] is listed in **Table 1**. The error of different numerical methods as compared to the experimental data is also compared in **Table 1**. An excellent agreement with a low error between the obtained values and those reported in the literature is found.
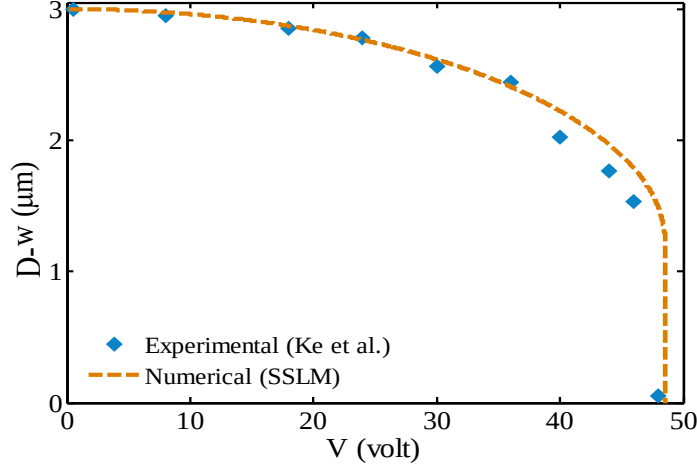
**Fig. 2.** Comparison of experimental [49] and numerical results for the cantilever wire (*D-w*: distance between the beam tip and the substrate)

**Table 1.** Comparison of the instability voltage (volt) of the numerical results with respect to experimentally measured values

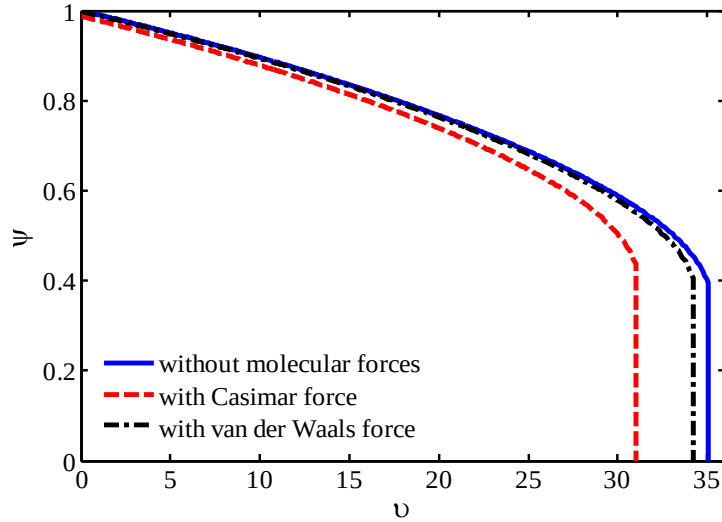| | Experiment [49] | FDM [50] | MAD [50] | MIM [51] | MVIM [51] | ROM [52] | HPM [53] | DQM [53] | SSLM (present) |
|---|---|---|---|---|---|---|---|---|---|
| Voltage | 48 | 47.1 | 47.08 | 51.15 | 47.74 | 47.4 | 48.33 | 49.57 | 48.51 |
| Error % | - | 1.88 | 1.92 | 6.56 | 0.54 | 1.25 | 0.69 | 3.27 | 1.06 |



**Fig. 3.** The effects of dispersion forces on the beam tip gap versus applied voltage (υ: nondimensional voltage parameter and $\psi$: nondimensional distance between the beam tip and the substrate)

In the following, the impacts of molecular forces and nonlinear curvature on the structural response of cantilever nanowires are assessed. The Young's modulus and wire diameter are chosen to be 1 TPa and 6 nm, respectively. The parameter $\upsilon$ denotes the nondimensional voltage parameter, see Eq. (35), and $\psi$ indicates the nondimensional distance between the beam tip and the substrate. Note that the following analyses will be carried out by considering N = 3.

The coupled effects of molecular attractions on the structural response of a microcantilever with the nondimensional terms ,$0=\beta,0=\alpha,72=\chi,1=\mu$ and $0=\kappa$ are examined in **Fig. 3**. It can be deduced

that ignoring the dispersion forces in the miniature devices may cause inaccurate responses. Accordingly, the predicted pull-in voltage without consideration of such forces will be more than that with consideration of them. In the ultra-small scale, both Casimir and vdW regimes possibly will be considerable; however, their effects are negligible in the macro-scale. In the present case, the Casimir effect on the system stability is more noteworthy due to the geometric conditions. Consequently, the vdW effect will be ignored in the investigation of this microsystem. Note that the vdW regime may be dominant in different circumstances, especially other gaps of conductors.

In **Fig. 4**, the relationship between beam deflections and the voltage parameter for different values of dimensionless nonlinear curvature parameter $\mu$ (square of initial gap-length ratio) are investigated. The results illustrate that the geometrical nonlinearity affects the critical voltage parameter significant, which results in increasing the structural stiffness. Consequently, the critical voltage of the linear model ($0=\mu$) is less than that with consideration of the nonlinearity. In addition, when the term $\mu$ decreases, the responses approach to those of the linear model. On the other hand, the effect of the Casimir regime on the obtained results is more evident with considering and enhancing the geometrical nonlinearity. Hence, by considering the molecular force, the difference of threshold voltages increases by an increase in the nonlinear deformation. Moreover, by considering the geometrical nonlinearity, the deflection of the cantilever tip increases. This point is essential in devices with a considerable primary gap to length ratio.

The relationship between the microbeam deflections and the electric potential for different cases of the nondimensional geometrical term $\chi$ (initial gap-radius ratio) are examined in **Fig. 5**. The acquired results reveal that an increase in this term results in the beam behaving stiffer and increases the threshold electric potential. In addition, the influence of geometrical nonlinearity on the structural behavior is more remarkable for large values of this parameter. It means that as the gap-radius ratio enhances, the difference between the threshold results increases by considering the nonlinearity. As a result, the responses of linear and nonlinear models will converge by considering an increase in the electrode diameter and decreasing the initial gap.

**Fig. 6** displays the variation of the wire deflection versus the external voltage by considering the residual surface effect in addition to the Casimir regime. The dimensionless parameter of the residual tension of surface layer is denoted by $\beta$. **Fig. 6** demonstrates that modeling the SL has a considerable impact on the system response and the difference between deflections with considering this parameter is remarkable. This point is explained by considering the stiffness relationship ($\beta K_3 + \mu K_4/2$) caused by the surface tension, which influences the structural behavior, especially in systems with a relatively considerable initial gap-length ratio. For the residual stress with the positive sign, the threshold voltage is lower than the one calculated without consideration of it, and vice versa. As a result, by considering the positive/negative surface tension, the stiffness of the cantilever microswitch can be decreased/increased. These observed behaviors in such systems meet the reported experimental [54] and analytical results [55]. Moreover, if we had neglected the nonlinear effect, the pull-in instability voltage would have been slightly lower.

The influence of the deflection curves on the voltage parameter, considering different surface elastic modulus are demonstrated in **Fig. 7**, where the dimensionless surface elastic parameter is denoted by $\alpha$. The influence of layer elasticity on structural stability is significant as the layer-induces tension effect. It is revealed that accounting the SL effect increases the microstructure stiffness, and thus increases the threshold voltage, unlike the positive residual surface tension effect. This result can also be understood by using the relationship of beam stiffness $K_1(1+\alpha)$. Moreover, the critical voltage enhances with increasing the nonlinearity as well as the SL elasticity. This point is explained by considering the relationship of nonlinear stiffness $2\mu K_2(1+\alpha)$.
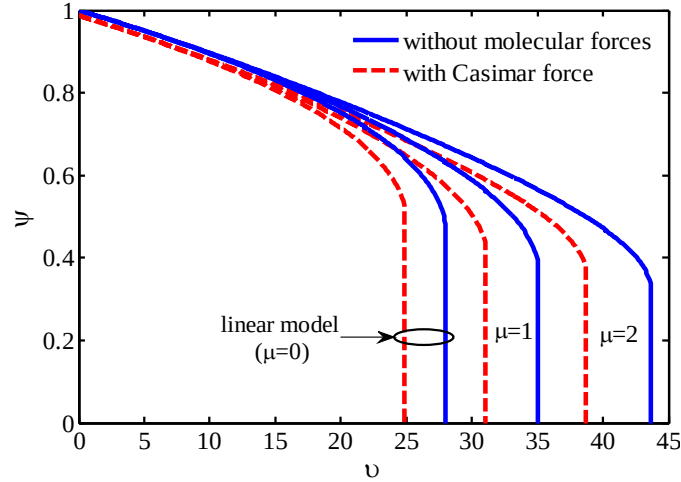
**Fig. 4.** The coupled effects of nonlinear curvature and molecular force on the beam tip gap ($\mu$: dimensionless nonlinear curvature parameter)
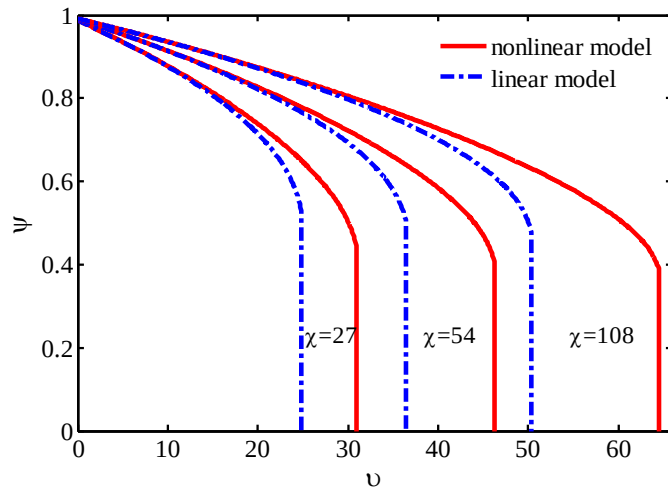


**Fig. 5.** The coupled effects of nonlinear curvature and geometrical parameter on the beam gap ($\chi$: nondimensional geometrical term)
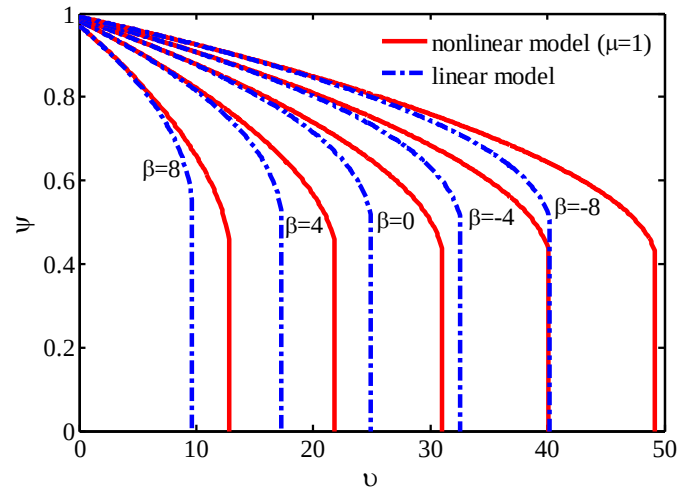


**Fig. 6.** The effects of positive and negative residual stress of SL on the beam tip gap ($\beta$: dimensionless parameter of the residual tension of surface layer)
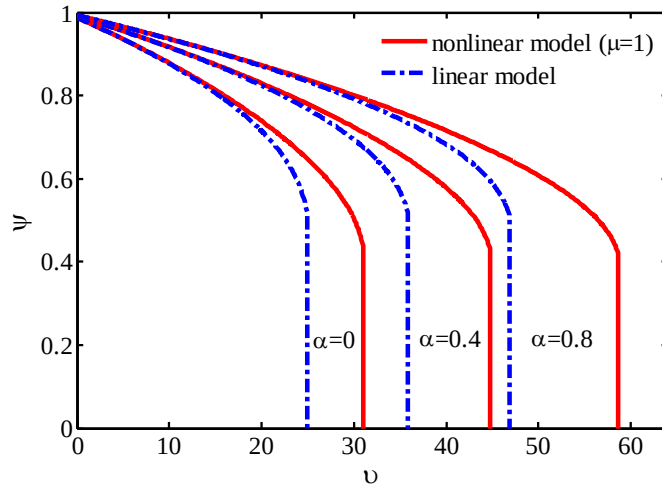
**Fig. 7.** The effects of SL elasticity on the beam tip gap ($\alpha$: dimensionless surface elastic parameter)
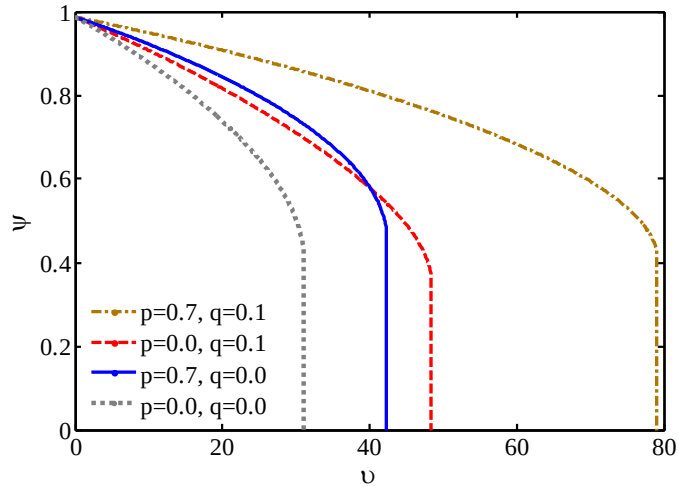


**Fig. 8.** The effects of non-actuated pieces of the substrate on the beam tip gap ($p$ and $q$: first and second dimensionless actuated length of the substrate, respectively)

    **Fig. 8** displays the relationship between the beam tip and electrostatic actuation by considering different conditions for the non-actuated area of the substrate. In general, the threshold voltage of a system with the partly actuated fixed conductor is more significant than an ordinary plate, which makes instability with a delay. Accordingly, the critical voltage enhances with an increase of parameters $p$ and $q$ (first and second dimensionless actuated length of the substrate, respectively). Moreover, the effect of the non-actuated second (end) area is more considerable than the first area. In other words, an increase in the applied electric potential has a more considerable effect when the parameter $q$ is increased. In addition, the effect of each non-actuated length on the critical voltage will be more noticeable when the other non-actuated piece is considered as well. This point agrees with the reported results for rectangular cantilever beams [56]. It is interesting to note that, the tip deflection of the microcantilever decreases with an increase in the dimension of the non-actuated base piece. This is a useful guideline, especially in the identification of system behavior and applied design of several sensors and switches.

12

The effect of the electric potential of microcantilevers on electrodes gap with assumptions of $q = 0$ and $p = 0$ are demonstrated in **Fig. 9** (a) and (b), respectively. It can be concluded that the impact of the Casimir regime on the instability characteristics will be stronger by restricting the electrically actuated pieces. Consequently, extending the tip part makes a crucial difference between the threshold voltage parameter by taking the molecular forces into account. In addition, this issue may not be seen clearly by changing the first piece dimension. It is worth noting that by setting, for example, $q = 0.26$ and without consideration of Casimir regime, the collapse will not be seen. Nevertheless, taking the Casimir force into account leads to much lower critical $\upsilon$. Another significant point is that by developing the base piece, the deformation of the tip beam decreases, however, the result of expanding the tip non-actuated piece is completely opposite. Finally, the influences of both pieces on the threshold characteristics do not change linearly, which specifies the importance of numerical analysis in such systems.
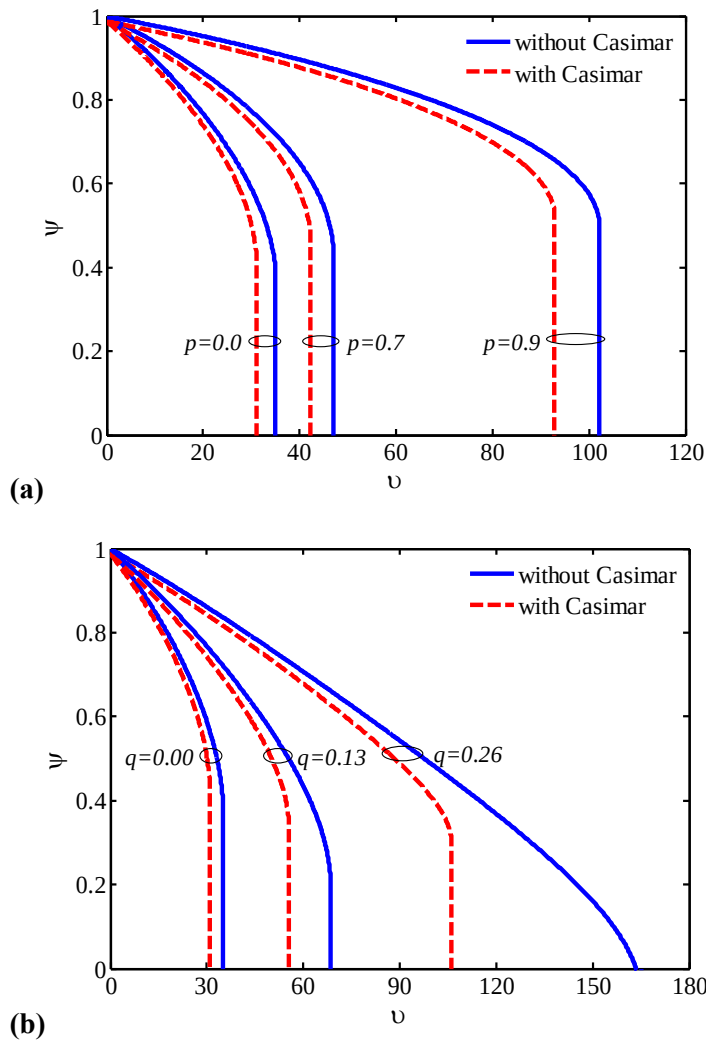


(a)



(b)

**Fig. 9.** The coupled effects of Casimir force and non-actuated piece of substrate on the beam tip gap; **(a)** $q = 0$, **(b)** $p = 0$

The effect of piezoelectric actuation $V_P$ on the structural stability of smart MEMS using linear and nonlinear models is investigated in **Fig. 10**. The results illustrate that piezoelectric excitation

13

affects the system responses significantly by shifting the equilibrium manifolds and instability conditions. It is possible to increase/decrease the threshold $\upsilon$ by considering positive/negative piezoelectric actuation. In this condition, the negative piezo-voltage produces an axial compression force, which results in a decrease in the stiffness of such piezobeams. This idea can be seen in both of the linear and nonlinear models by applying a relatively low piezo-voltage. This is an important application of smart microsystems in various devices that must have low energy consumption.

Another noteworthy phenomenon that may be seen in small-scale devices is freestanding, which means that the deformable part faces an initial deflection, while there is no external electric potential. For an electrode with known geometrical properties, it should be considered a minimum primary distance to make certain that it does not stick on the ground conductor without applying the electrostatic load, especially by taking the molecular effects into account. Moreover, this phenomenon becomes more obvious by applying the negative piezoelectric actuation because it causes remarkable initial deflection at zero DC voltage. Consequently, we would be able to apply the piezoelectric excitation as a design factor in smart manipulators to avoid occurring instability.

**Fig. 11** depicts the effects of piezoelectricity on the threshold characteristics of smart instruments with consideration of nonlinear curvature quantitatively and qualitatively. It can be concluded that by applying and increasing the positive piezo-voltage, the threshold voltage increases significantly in both linear and nonlinear models. Moreover, the difference between the critical electric potential at different signs and values of the piezo-voltage will be constant in the two mentioned models. On the other hand, the effect of piezo-voltage variations on the displacement of the beam end is completely different, where the parameter $\Upsilon$ denotes the dimensionless vertical displacement of the beam tip. As illustrated in **Fig. 11** b, the results of models converge gradually because the results of linear (nonlinear) model increase (decrease) with increasing the piezoelectric voltage. As a result, considering the linear or nonlinear model considerably affects the predicted values for the deflection of the movable beam with consid[...]by applying a negative piezo-voltage.
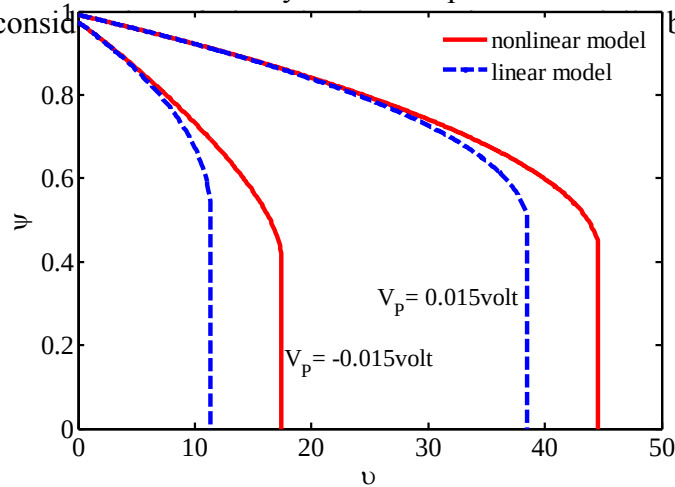


**Fig. 10.** The coupled effects of piezoelectric and electrostatic actuations on the beam tip gap
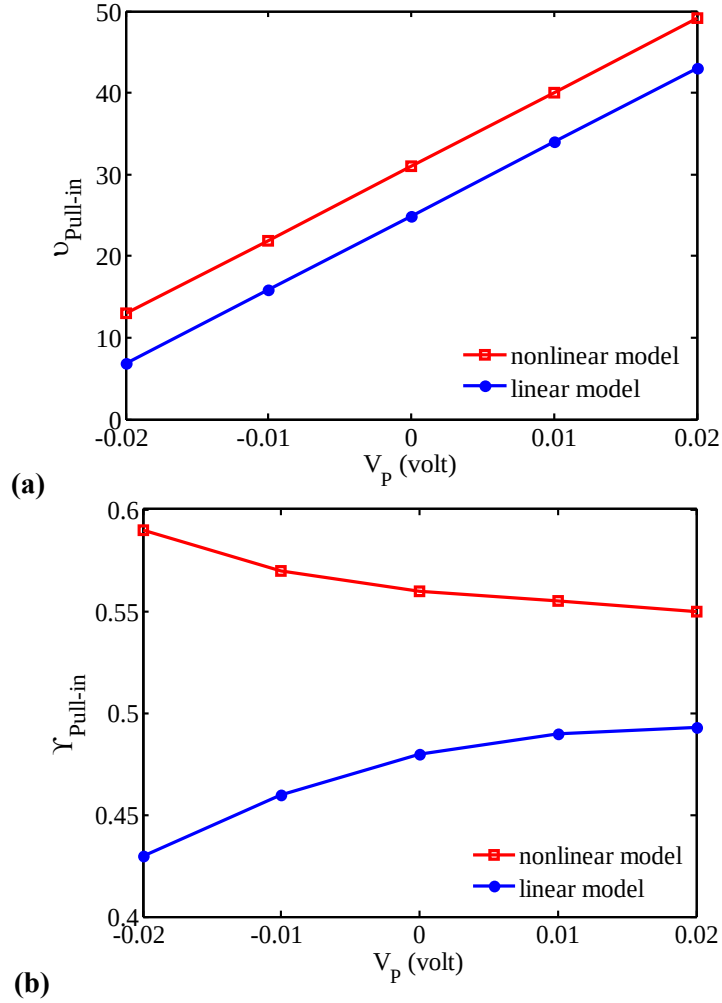
**Fig. 11.** The coupled effects of nonlinear curvature in addition to piezoelectric and electrostatic actuations on the **(a)** threshold voltage, **(b)** beam deflection ($\Upsilon$: dimensionless vertical displacement of the beam tip)

The coupled influences of the electrically non-actuated pieces of the substrate plate in addition to the piezoelectric and electrostatic actuations on the behaviors of the smart system are investigated in **Fig. 12**. A review of the figure reveals that the effect of the non-actuated piece becomes more/less remarkable by applying the positive/negative piezo-voltage. Hence, the difference between the curves by considering the non-actuated piece increases by applying a positive voltage, especially by considering the second non-actuated piece, see **Fig. 12** b. Moreover, expanding the non-actuated tip piece not only enhances the critical voltage extremely but also results in a considerable increase in the threshold deflection, especially with consideration of the positive piezoelectricity. Accordingly, considering the appropriate configuration seems essential in the design of piezoelectric micro and nanosystems to reach the expected goals.
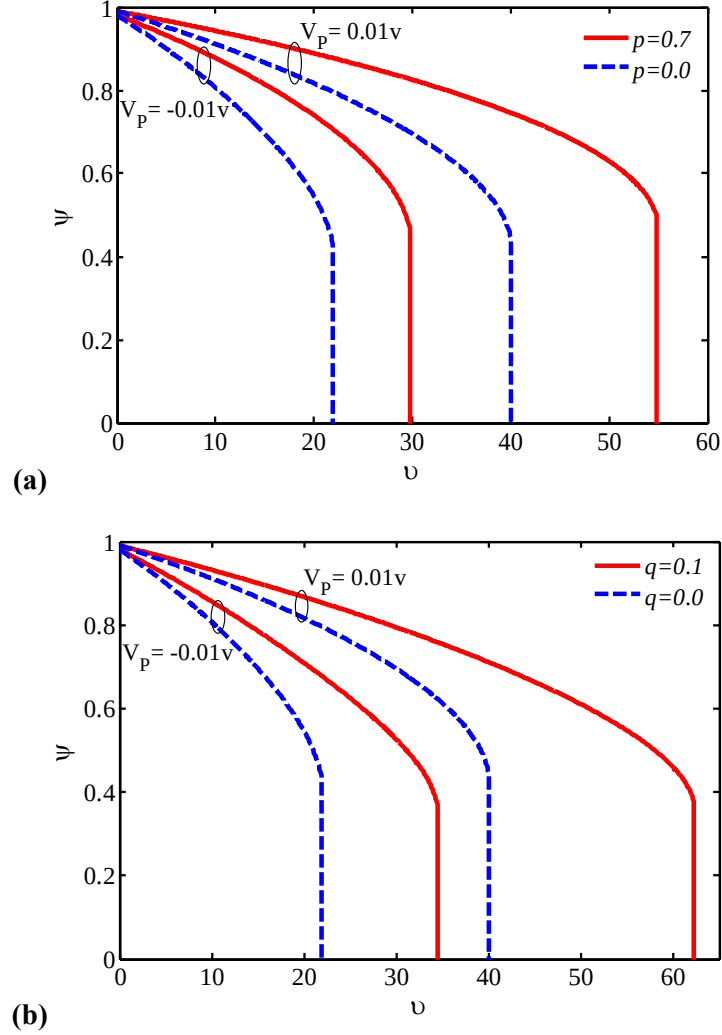
**Fig. 12.** The coupled effects of non-actuated pieces of substrate in addition to piezoelectric and electrostatic actuations on the beam tip gap; **(a)** $q \ 0 =$, **(b)** $p \ 0 =$

## 5. Conclusion

The main goal of this research was to present a versatile smart MEMS with the capability of adjusting stability conditions to improve the system characteristics. The proper adjustments were implemented by applying the piezo-voltage and/or actuating just a piece of the substrate electrostatically. The coupled influences of dispersion forces, material length-scale, surface layer, and geometrical nonlinearity were included in the present model. To improve the properties of the system such as controllability and tuning applications, only a part of the fixed plate was electrostatically actuated. The obtained results were validated with available experimental and numerical results.

It was found that the Casimir regime affects the system response remarkably. Nevertheless, the pull-in phenomenon may not occur when ignoring it, so the critical voltage would be overestimated dramatically. Moreover, the deformable wire may experience an initial deflection at zero voltage that causes undesirable adhesion in the freestanding. The results showed that considering the nonlinear curvature increases the beam deflection and voltage. Furthermore, taking into account

16

the non-actuated tip piece increases the critical voltage and deformation, however, considering the non-actuated base piece results in decreasing the pull-in deflection.

Performing real-time experiments to demonstrate the effectiveness of the proposed method could be considered in the future, which is beyond the scope of this research work. Several representative nanostructures such as controllable switches and sensors/ actuators were incorporated in the present model.

### Declaration of conflicting interests

The authors declared no potential conflicts of interest in preparing this article.

### References

[1] M. Fakher, S. Rahmanian, S. Hosseini-Hashemi, On the carbon nanotube mass nanosensor by integral form of nonlocal elasticity, International Journal of Mechanical Sciences, 150 (2019) 445-457.

[2] F. Tavakolian, A. Farrokhabadi, M. SoltanRezaee, S. Rahmanian, Dynamic pull-in of thermal cantilever nanoswitches subjected to dispersion and axial forces using nonlocal elasticity theory, Microsystem Technologies, 25 (2019) 19-30.

[3] M. SoltanRezaee, M. Afrashi, S. Rahmanian, Vibration analysis of thermoelastic nano-wires under Coulomb and dispersion forces, International Journal of Mechanical Sciences, 142-143 (2018) 33-43.

[4] A.E. Mamaghani, S.E. Khadem, S. Bab, S.M. Pourkiaee, Irreversible passive energy transfer of an immersed beam subjected to a sinusoidal flow via local nonlinear attachment, International Journal of Mechanical Sciences, 138 (2018) 427-447.

[5] M. SoltanRezaee, A. Farrokhabadi, M.R. Ghazavi, The influence of dispersion forces on the size-dependent pull-in instability of general cantilever nano-beams containing geometrical non-linearity, International Journal of Mechanical Sciences, 119 (2016) 114-124.

[6] A. Mohebshahedin, A. Farrokhabadi, The influence of the surface energy on the instability behavior of NEMS structures in presence of intermolecular attractions, International Journal of Mechanical Sciences, 101 (2015) 437-448.

[7] A. Farrokhabadi, A. Mohebshahedin, R. Rach, J.-S. Duan, An improved model for the cantilever NEMS actuator including the surface energy, fringing field and Casimir effects, Physica E: Low-dimensional Systems and Nanostructures, 75 (2016) 202-209.

[8] L.L. Silva, M.A. Savi, P.C. Monteiro, T.A. Netto, On the nonlinear behavior of the piezoelectric coupling on vibration-based energy harvesters, Shock and Vibration, 2015 (2015).

[9] S. Kamarian, M. Shakeri, M. Yas, M. Bodaghi, A. Pourasghar, Free vibration analysis of functionally graded nanocomposite sandwich beams resting on Pasternak foundation by considering the agglomeration effect of CNTs, Journal of Sandwich Structures & Materials, 17 (2015) 632-665.

[10] M. SoltanRezaee, M.R. Ghazavi, Thermal, size and surface effects on the nonlinear pull-in of small-scale piezoelectric actuators, Smart Materials and Structures, 26 (2017) 095023.

[11] R.P. Jenkins, M. Ivantysynova, A lumped parameter vane pump model for system stability analysis, International Journal of Hydromechatronics, 1 (2018) 361-383.

[12] M. SoltanRezaee, M.-R. Ghazavi, A. Najafi, Parametric resonances for torsional vibration of excited rotating machineries with nonconstant velocity joints, Journal of Vibration and Control, 24 (2018) 3262-3277.

[13] R. Kolahchi, B. Keshtegar, Buckling and reliability analysis of CNT-reinforced-beams based on Hasofer-Lind and Rackwitz-Fiessler methods, International Journal of Hydromechatronics, 1 (2018) 403-414.

[14] R. Ai, L.L.S. Monteiro, P.C.C. Monteiro, P.M.C.L. Pacheco, M.A. Savi, Piezoelectric Vibration-Based Energy Harvesting Enhancement Exploiting Nonsmoothness, Actuators, 8 (2019) 25.

[15] T.L. Pereira, A.S. de Paula, A.T. Fabro, M.A. Savi, Random effects in a nonlinear vibration-based piezoelectric energy harvesting system, International Journal of Bifurcation and Chaos, 29 (2019) 1950046.

[16] S.K. Lamoreaux, The Casimir force: background, experiments, and applications, Reports on progress in Physics, 68 (2005) 201.

[17] P. Ganguly, G.R. Desiraju, Van der Waals and polar intermolecular contact distances: Quantifying supramolecular synthons, Chemistry–An Asian Journal, 3 (2008) 868-880.

[18] J.B. Ma, L. Jiang, S.F. Asokanthan, Influence of surface effects on the pull-in instability of NEMS electrostatic switches, Nanotechnology, 21 (2010) 505708.

[19] W.D. Yang, F.P. Yang, X. Wang, Dynamic instability and bifurcation of electrically actuated circular nanoplate considering surface behavior and small scale effect, International Journal of Mechanical Sciences, 126 (2017) 12-23.

[20] S. Esfahani, S.E. Khadem, A.E. Mamaghani, Nonlinear vibration analysis of an electrostatic functionally graded nano-resonator with surface effects based on nonlocal strain gradient theory, International Journal of Mechanical Sciences, 151 (2019) 508-522.

[21] S. Rahmanian, S. Hosseini-Hashemi, Size-dependent resonant response of a double-layered viscoelastic nanoresonator under electrostatic and piezoelectric actuations incorporating surface effects and Casimir regime, International Journal of Non-Linear Mechanics, 109 (2019) 118-131.

[22] S. Rahmanian, M.-R. Ghazavi, S. Hosseini-Hashemi, On the numerical investigation of size and surface effects on nonlinear dynamics of a nanoresonator under electrostatic actuation, Journal of the Brazilian Society of Mechanical Sciences and Engineering, 41 (2019) 16.

[23] J. Shen, H. Wang, S. Zheng, Size-dependent pull-in analysis of a composite laminated micro-beam actuated by electrostatic and piezoelectric forces: Generalized differential quadrature method, International Journal of Mechanical Sciences, 135 (2018) 353-361.

[24] D.C.C. Lam, F. Yang, A. Chong, J. Wang, P. Tong, Experiments and theory in strain gradient elasticity, Journal of the Mechanics and Physics of Solids, 51 (2003) 1477-1508.

[25] A.W. McFarland, J.S. Colton, Role of material microstructure in plate stiffness with relevance to microcantilever sensors, Journal of Micromechanics and Microengineering, 15 (2005) 1060.

[26] U.B. Ejike, The plane circular crack problem in the linearized couple-stress theory, International Journal of Engineering Science, 7 (1969) 947-961.

[27] A.C. Eringen, D. Edelen, On nonlocal elasticity, International Journal of Engineering Science, 10 (1972) 233-248.

[28] T. Anderson, A. Nayfeh, B. Balachandran, Experimental verification of the importance of the nonlinear curvature in the response of a cantilever beam, Journal of Vibration and Acoustics, 118 (1996) 21-27.

[29] H. Dai, D. Zhao, J. Zou, L. Wang, Surface effect on the nonlinear forced vibration of cantilevered nanobeams, Physica E: Low-dimensional Systems and Nanostructures, 80 (2016) 25-30.

[30] P. Firoozy, S.E. Khadem, S.M. Pourkiaee, Power enhancement of broadband piezoelectric energy harvesting using a proof mass and nonlinearities in curvature and inertia, International Journal of Mechanical Sciences, 133 (2017) 227-239.

[31] J. Fang, J. Gu, H. Wang, Size-dependent three-dimensional free vibration of rotating functionally graded microbeams based on a modified couple stress theory, International Journal of Mechanical Sciences, 136 (2018) 188-199.

[32] S.M. Pourkiaee, S.E. Khadem, M. Shahgholi, Parametric resonances of an electrically actuated piezoelectric nanobeam resonator considering surface effects and intermolecular interactions, Nonlinear Dynamics, 84 (2016) 1943-1960.

[33] S.M. Pourkiaee, S.E. Khadem, M. Shahgholi, Nonlinear vibration and stability analysis of an electrically actuated piezoelectric nanobeam considering surface effects and intermolecular interactions, Journal of Vibration and Control, 23 (2017) 1873-1889.

[34] M. SoltanRezaee, M. Afrashi, Modeling the nonlinear pull-in behavior of tunable nano-switches, International Journal of Engineering Science, 109 (2016) 73-87.

[35] A. Shoghmand, M.T. Ahmadian, Dynamics and vibration analysis of an electrostatically actuated FGM microresonator involving flexural and torsional modes, International Journal of Mechanical Sciences, 148 (2018) 422-441.

[36] A. Nikpourian, M.R. Ghazavi, S. Azizi, On the nonlinear dynamics of a piezoelectrically tuned micro-resonator based on non-classical elasticity theories, International Journal of Mechanics and Materials in Design, 14 (2018) 1-19.

[37] A. Kazemi, R. Vatankhah, M. Farid, Nonlinear pull-in instability of microplates with piezoelectric layers using modified couple stress theory, International Journal of Mechanical Sciences, 130 (2017) 90-98.

[38] H. Li, X. Wang, J. Chen, Nonlinear electro-mechanical coupling vibration of corrugated graphene/piezoelectric laminated structures, International Journal of Mechanical Sciences, 150 (2019) 705-714.

[39] F. Yang, A. Chong, D.C.C. Lam, P. Tong, Couple stress based strain gradient theory for elasticity, International Journal of Solids and Structures, 39 (2002) 2731-2743.

[40] S. Kong, S. Zhou, Z. Nie, K. Wang, The size-dependent natural frequency of Bernoulli–Euler micro-beams, International Journal of Engineering Science, 46 (2008) 427-437.

[41] H. Georgiadis, E. Velgaki, High-frequency Rayleigh waves in materials with micro-structure and couple-stress effects, International Journal of Solids and Structures, 40 (2003) 2501-2520.

[42] D.H. Hodges, Proper definition of curvature in nonlinear beam kinematics, AIAA journal, 22 (1984) 1825-1827.

[43] B. Gheshlaghi, S.M. Hasheminejad, Vibration analysis of piezoelectric nanowires with surface and small scale effects, Current Applied Physics, 12 (2012) 1096-1099.

[44] M. Li, R.B. Bhiladvala, T.J. Morrow, J.A. Sioss, K.-K. Lew, J.M. Redwing, C.D. Keating, T.S. Mayer, Bottom-up assembly of large-area nanowire resonator arrays, Nature Nanotechnology, 3 (2008) 88-92.

[45] T. Emig, R. Jaffe, M. Kardar, A. Scardicchio, Casimir interaction between a plate and a cylinder, Physical review letters, 96 (2006) 080403.

[46] D. Marc, S.V. Rotkin, N.R. Aluru, Calculation of pull-in voltages for carbon-nanotube-based nanoelectromechanical switches, Nanotechnology, 13 (2002) 120.

[47] J.-G. Guo, Y.-P. Zhao, Dynamic stability of electrostatic torsional actuators with van der Waals effect, International Journal of Solids and Structures, 43 (2006) 675-685.

[48] K. Rashvand, G. Rezazadeh, H. Mobki, M.H. Ghayesh, On the size-dependent behavior of a capacitive circular micro-plate considering the variable length-scale parameter, International Journal of Mechanical Sciences, 77 (2013) 333-342.

[49] C.-H. Ke, N. Pugno, B. Peng, H. Espinosa, Experiments and modeling of carbon nanotube-based NEMS devices, Journal of the Mechanics and Physics of Solids, 53 (2005) 1314-1333.

[50] J. Mokhtari, A. Farrokhabadi, R. Rach, M. Abadyan, Theoretical modeling of the effect of Casimir attraction on the electrostatic instability of nanowire-fabricated actuators, Physica E: Low-dimensional Systems and Nanostructures, 68 (2015) 149-158.

[51] A. Koochi, A. Farrokhabadi, M. Abadyan, Modeling the size dependent instability of NEMS sensor/actuator made of nano-wire with circular cross-section, Microsystem Technologies, 21 (2015) 355-364.

[52] M. Keivani, M. Mardaneh, A. Koochi, M. Rezaei, M. Abadyan, On the dynamic instability of nanowire-fabricated electromechanical actuators in the Casimir regime: Coupled effects of surface energy and size dependency, Physica E: Low-dimensional Systems and Nanostructures, 76 (2016) 60-69.

[53] M. Keivani, A. Koochi, H.M. Sedighi, M. Abadyan, A. Farrokhabadi, A.M. Shahedin, Effect of Surface Layer on Electromechanical Stability of Tweezers and Cantilevers Fabricated from Conductive Cylindrical Nanowires, Surface Review and Letters, 23 (2016) 1550101.

[54] S.G. Nilsson, X. Borrise, L. Montelius, Size effect on Young's modulus of thin chromium cantilevers, Applied physics letters, 85 (2004) 3555.

[55] J. He, C.M. Lilley, Surface effect on the elastic behavior of static bending nanowires, Nano Letters, 8 (2008) 1798-1802.

[56] K. Wang, B. Wang, A general model for nano-cantilever switches with consideration of surface effects and nonlinear curvature, Physica E: Low-dimensional Systems and Nanostructures, 66 (2015) 197-208.